Developmental Biology 449 (2019) 107–114

Contents lists available at ScienceDirect

Developmental Biology

journal homepage: www.elsevier.com/locate/developmentalbiology

Neural crest state activation in NRAS driven melanoma, but not in NRAS-driven melanocyte expansion

Alicia M. McConnell[a,b,c], Jeffrey K. Mito[a,b,c,d], Julien Ablain[a,b,c], Michelle Dang[a,b,c], Luke Formichella[a,b,c], David E. Fisher[c,e], Leonard I. Zon[a,b,c,*]

[a] Stem Cell Program and Division of Hematology/Oncology, Children's Hospital Boston, Howard Hughes Medical Institute, Boston, MA 02115, USA
[b] Harvard Stem Cell Institute, Boston, MA 02115, USA
[c] Harvard Medical School, Boston, MA 02115, USA
[d] Department of Pathology, Brigham and Women's Hospital, Boston, MA 02215, USA
[e] Cutaneous Biology Research Center, Massachusetts General Hospital, Charlestown, MA 02129, USA

ARTICLE INFO

Keywords:
Neural crest
Melanoma
Cancer
NRAS

ABSTRACT

NRAS mutations are frequently found in many deadly malignancies and are the second most common oncogene driving malignant melanoma. Here, we generate a rapid transient transgenic zebrafish model of $NRAS^{Q61R}$-mutant melanoma. These fish develop extensive melanocytic proliferation in approximately 4 weeks. The majority of these lesions do not engraft upon transplantation and lack overt histologic features of malignancy. Our previous work demonstrated that activation of a neural crest cell transcriptional program is a key initiating event in zebrafish BRAF/p53-driven melanomas using the fluorescent reporter *crestin:EGFP*. By 8–12 weeks of age, some lesions progress to malignant melanoma and have cytologic atypia, destructive tissue invasion, and express neural crest progenitor markers, including *crestin:EGFP*. Our studies demonstrate that $NRAS^{Q61R}$ induces extensive melanocyte expansion, which arise during zebrafish development and lack a transformed phenotype. These early lesions are highly predisposed to reactivate a neural crest progenitor fate and form malignant melanomas.

1. Introduction

Although melanoma only accounts for about 1% of skin cancers in the United States, it is responsible for 60–80% of skin cancer related deaths (Siegel et al., 2016). Mutations in the NRAS oncogene occur in about 30% of patients with melanoma and, of these, 40% have a Q61R hot-spot mutation (Akbani et al., 2015). Furthermore, patients with *NRAS* or *BRAF* mutations have significantly shorter survival compared to patients without these mutations and are more likely to have central nervous system involvement compared to *NRAS/BRAF* wild type patients (Jakob et al., 2012). Recently, a phase 3 clinical trial was completed showing that the MEK inhibitor binimetinib improved progression-free, but not overall, survival in patients with *NRAS*-mutated melanoma (Dummer et al., 2017). In general, immunotherapies and MEK pathway inhibitors have improved overall patient survival (Johnson and Puzanov, 2015); however, careful characterization of tumor initiation and progression is needed to develop novel therapeutic targets, particularly for *NRAS*-mutant melanoma.

Melanoma arises due to a malignant transformation of melanocytes, which are embryonically derived from the neural crest. Our lab has previously generated two zebrafish models of melanoma that display histological and molecular characteristics of human melanomas: $mitfa{:}BRAF^{V600E};p53^{-/-}$ and $mitfa{:}EGFP{:}NRAS^{Q61K};p53^{-/-}$ (Dovey et al., 2009; Patton et al., 2005). $mitfa{:}BRAF^{V600E};p53^{-/-}$ zebrafish melanomas were shown to activate a neural crest progenitor gene signature, which was also expressed in human melanomas (Kaufman et al., 2016; Rambow et al., 2015; White et al., 2011). One gene, *crestin*, is expressed in neural crest progenitor cells, which turns off after 3 days, and then turns on again specifically in melanomas. By using the *crestin* promoter/enhancer to drive EGFP, neural crest progenitor state reactivation and tumor initiation could be visualized in mutant BRAF zebrafish (Kaufman et al., 2016). However, the reemergence of neural crest progenitor state in other genotypes, such as *NRAS*-mutant melanoma, has not been explored.

In this study, we generated a rapid transient transgenic zebrafish model of melanoma by overexpressing $NRAS^{Q61R}$ in melanocytes (abbreviated *mcr:NRAS*). We found that the *mcr:NRAS* fish develop large melanocyte proliferations around 4 weeks post fertilization. These

* Corresponding author at: Stem Cell Program and Division of Hematology/Oncology, Children's Hospital Boston, Howard Hughes Medical Institute, Boston, MA 02115, USA.
E-mail address: zon@enders.tch.harvard.edu (L.I. Zon).

https://doi.org/10.1016/j.ydbio.2018.05.026
Received 21 December 2017; Received in revised form 30 May 2018; Accepted 30 May 2018
Available online 05 June 2018
0012-1606/

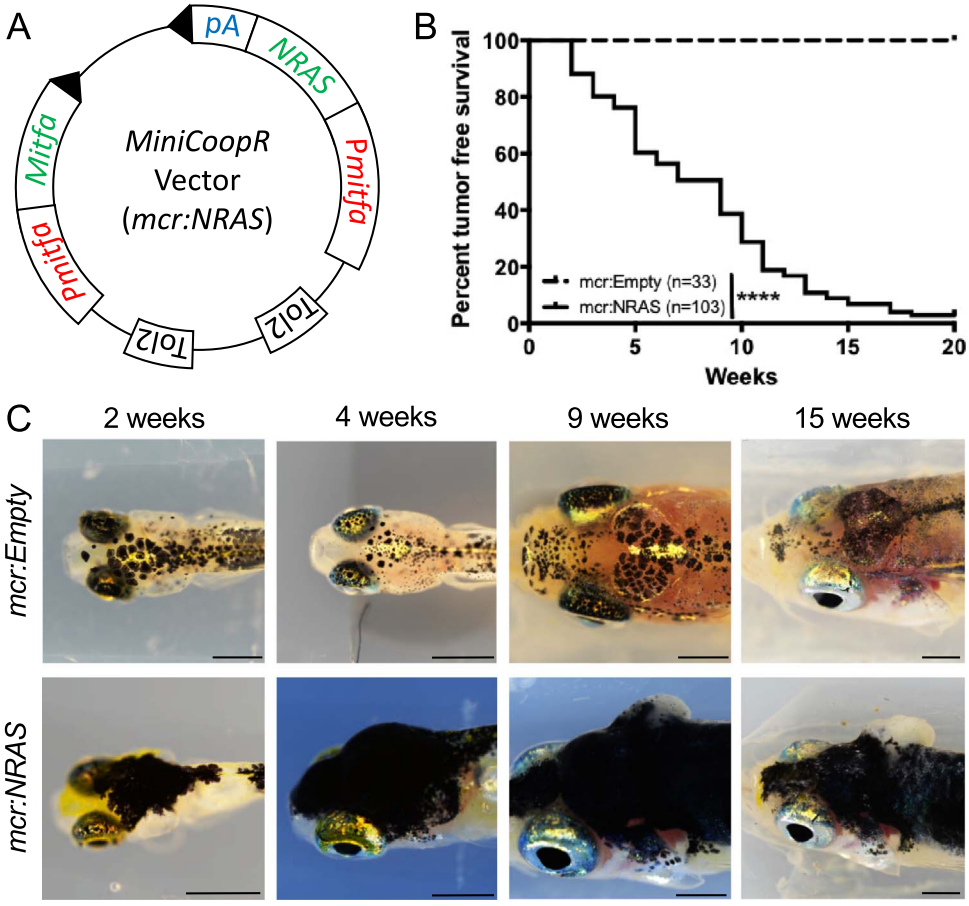

Fig. 1. Zebrafish model of *NRAS*-driven melanoma. (A) Schematic of the *MiniCoopR* vector containing the $NRAS^{Q61R}$ gene driven by the *mitfa* promoter (*Pmitfa*) in cis with the *mitfa* gene. (B) Kaplan-Meier curve showing the percent of *casper;mcr:NRAS* zebrafish without grossly apparently tumors compared to *casper;mcr:Empty* fish. ****$p < 0.0001$ calculated using the log rank Mantel-Cox test. (C) Images of *casper;mcr:NRAS* and *casper mcr:Empty* fish taken at 2, 4, 9, and 15 weeks post fertilization. In contrast to the tumor formation seen in the *casper;mcr:NRAS* fish, normal melanocyte patterning is observed in *casper;mcr:Empty* controls. Scale bars represent 500 μm for 2 week images and 1000 μm for 4–15 week images.

masses progress to malignant melanoma at 8–12 weeks post fertilization. Unlike the malignant melanoma seen in older *mcr:NRAS* fish, most 4 week tumors lack overt histologic features of malignancy and do not form tumors upon transplantation. Markers of neural crest progenitor cells are not expressed in the early tumors, but are expressed by the malignant melanomas. These results demonstrate a biphasic role for NRAS in melanocyte expansion and melanoma formation.

2. Results

2.1. A rapid zebrafish model of NRAS-driven melanoma

In order to rapidly model human melanoma in the zebrafish, we overexpressed $NRAS^{Q61R}$ using the *MiniCoopR* vector (*mcr:NRAS*). In this transposon-based transgenic system, *mitfa*, an essential gene in melanocytes, is linked in *cis* to $NRAS^{Q61R}$, also driven by the *mitfa* promoter (Fig. 1A) (Ceol et al., 2011; Kwan et al., 2007). When injected into *casper* ($mitfa^{-/-}$;$roy^{-/-}$) embryos, the *mcr:NRAS* vector not only rescues melanocytes, but also drives expression of $NRAS^{Q61R}$ in the rescued melanocytes. We assessed tumor formation in these fish compared to controls injected with an empty *MiniCoopR* vector (*mcr:Empty*) (White et al., 2008). We found that the *casper;mcr:NRAS* fish develop large hyperpigmented patches of melanocytes at around 2 weeks of age (Fig. 1C; Supp. Fig. 1A). By 4 weeks post fertilization, about 20% of these patches form masses that protrude above the body plane (Fig. 1B and C; Supp. Fig. 1B). After 8 weeks of age, rapid tumor onset occurs from within these patches (Fig. 1B and C; Supp. Fig. 1C and D). This tumor onset is greatly accelerated compared to the previously published stable $mitfa:BRAF^{V600E};p53^{-/-}$ and $mitfa:EGFP:NRAS^{Q61K};p53^{-/-}$ zebrafish, which occurs between 4 and 6 months of age (Dovey et al., 2009; Patton et al., 2005). Together, these data show that our zebrafish NRAS model induces rapid tumor development, without the assistance of a tumor suppressor.

2.2. Histologic characterization of mcr:NRAS melanoma

To characterize the nature of the melanocytic lesions developed in *mcr:NRAS* fish, representative tumors were evaluated by histology at 4, 8, and 20 weeks (Table 1). Among 16 fish with grossly apparent masses at 4 weeks, 10 had lesions similar to the F-nevi generated in $mitfa:BRAF^{V600E}$ fish (Patton et al., 2005) and 3 had indeterminate

Table 1
Histologic scoring of *casper;mcr:NRAS* zebrafish. Table displaying the fraction of samples from 4, 8, and 20 week old *casper;mcr:NRAS* zebrafish that fall into the following categories: indeterminate, nevus, melanocytic tumors of indeterminate potential (MTIP), or malignant melanoma.

Week	Tumor Type			
	Indeterminate	Nevus	MTIP	Melanoma
4	3/16	10/16	2/16	1/16
8	1/9	3/9	0/9	5/9
20	0/12	0/12	0/12	12/12

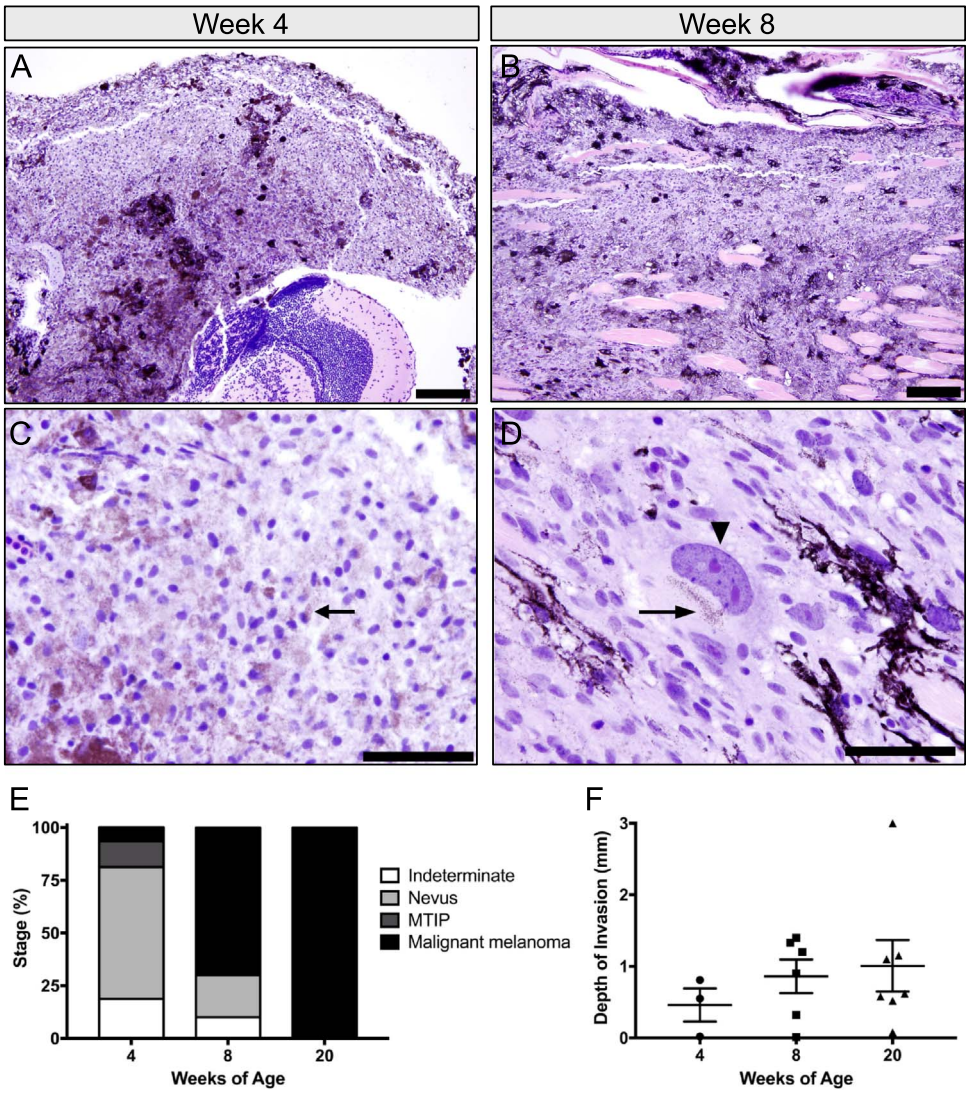

Fig. 2. Histologic analysis of *casper;mcr:NRAS* zebrafish. (A-D) H & E of *casper;mcr:NRAS* fish. (A and C) Melanocytic tumor of indeterminate potential (MTIP) at 4 weeks of age (original magnification 200 ×). High magnification image in C shows an epithelioid morphology with minimal cytologic atypia (original magnification 1000 ×). (B and D) Malignant melanoma collected at 8 weeks of age, showing infiltrative growth through underlying skeletal muscle (original magnification 200 ×). A high magnification image shows cytologically malignant cells with significant anisonucleosis and prominent nucleoli (original magnification 1000 ×). Arrowhead shows enlarged nuclei with prominent nucleoli and arrows show melanin pigment. Scale bars represent 50 μm for (A) and (B) and 20 μm for (C) and (D). (E) Tumors collected at 4, 8, and 20 weeks were scored as either indeterminate, nevus (F-nevi), MTIP, or malignant melanoma based on histological assessment. n = 9–16 (F) No significant difference in the depth of invasion from the basement membrane between 4, 8, and 20 week MTIP and melanomas (one-way ANOVA). n = 3–7.

lesions. Two of the 4 week old fish had large melanocytic tumors characterized by a pushing border that invaded underlying anatomic structures including skeletal muscle and the central nervous system of the fish (Fig. 2A; Supp. Fig. 2A). In contrast to tumors at later developmental ages, these two tumors lacked significant cytologic atypia, did not have an infiltrative growth pattern, and were thought to be morphologically distinct from both the F-nevi and malignant melanomas generated in *mitfa:BRAF*^{V600E} fish. Cells in these 4 week masses had an epithelioid morphology, with minimal cytologic atypia (Fig. 2C; Supp. Fig. 2C). Given the distinct cytologic and architectural growth pattern of these tumors, they were thought to be best classified as melanocytic tumors of indeterminate potential (MTIP). Additionally, one fish at 4 weeks had a superficially invasive malignant melanoma (Fig. 2E). The three tumors categorized as MTIP or malignant melanoma at 4 weeks had no significant difference in the depth of invasion compared to the malignant melanomas seen at 8 and 20 weeks (Fig. 2F). In contrast, tumors that arose at later time points (8 and 20 weeks) routinely showed overt histologic features of malignancy. Among the 9 fish evaluated at 8 weeks, 5 had malignant melanomas, including 1 fish with 3 distinct melanomas, and 3 had F-nevi. At 20 weeks, all 9 fish evaluated by histology had malignant melanoma, 3 of which had multiple melanomas (Fig. 2E). In contrast to tumors at 4 weeks, tumors at 8 and 20 weeks had an infiltrative growth pattern into the underlying tissue and significant cytologic atypia including marked nuclear enlargement and the presence of prominent nucleoli (Fig. 2B, and D; Supp. Fig. 2B and C). Activated MAPK signaling is typical in human nevi and melanomas (Uribe et al., 2006). Using immunohistochemistry, phospho-ERK expression was studied in 4, 8, and 20 *mcr:NRAS* tumors. We found that all tumors at 4, 8, and 20 weeks showed phospho-ERK staining, which indicates activated MAPK signaling (Supp. Fig. 3).

2.3. mcr:NRAS malignant melanoma engrafts upon transplantation

The ability for a cell to initiate tumors upon transplantation is a classic assay to test transformation. Therefore, we sought to determine if the early *mcr:NRAS* tumors can engraft and grow when transplanted. Tumors from 4 and 20 week old *mcr:NRAS* fish were homogenized,

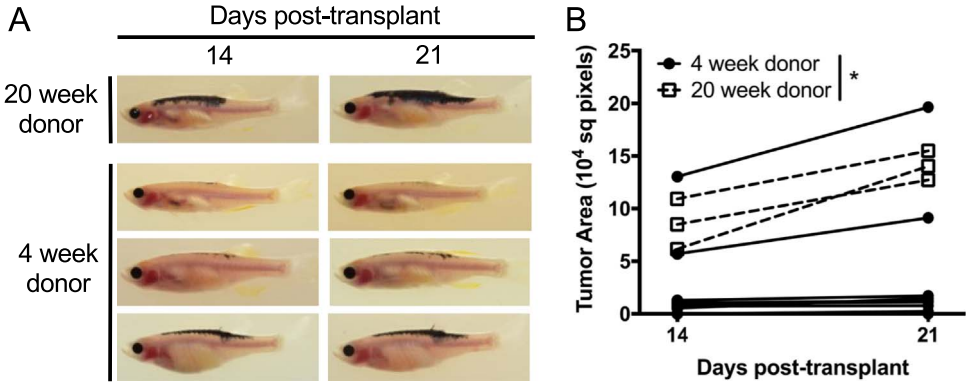

Fig. 3. 20 week *casper;mcr:NRAS* melanomas engraft upon transplantation. (A) Images of tumors in recipient fish at 14 and 21 days post-transplant. (B) 20 week *casper;mcr:NRAS* melanomas engraft significantly better upon transplantation than 4 week donors. *p = 0.0141 calculated by a two-way ANOVA. n = 3 and 11 for 20- and 4-week old donors respectively.

resuspended in PBS, and 100k tumor cells were injected into the dorsal cavity of age-matched, irradiated recipients. At both 14 and 21 days post-transplant, cells from the 20 week old donor engrafted and grew significantly more than the 4 week old donor (Fig. 3A and B; Supp. Fig. 4A). Only two of the eleven 4 week old *mcr:NRAS* donors were able to engraft, as compared to 100% of the three 20 week old donors (Supp. Fig. 4B), indicating that the majority of lesions present at 4 weeks are not capable of engraftment upon transplantation.

2.4. Neural crest progenitor signature in NRAS-driven melanoma

Given that the neural crest gene, *crestin*, is expressed in 100% of zebrafish *mitfa:BRAF^{V600E};p53$^{-/-}$* melanomas (Kaufman et al., 2016), we investigated whether the *NRAS*-driven melanomas also had a reactivated neural crest progenitor state. To do this, we injected the *mcr:NRAS* vector into the embryos of a stable line of *casper;crestin:EGFP* zebrafish and imaged at various ages to determine *crestin* onset. The *crestin:EGFP* transgene was off in all of the 4 week old masses evaluated (n = 30), but turned on between 9 and 12 weeks of age, occurring in the same time frame as histologic evidence of malignancy (Fig. 4). By 20 weeks of age, 100% of tumors present in *mcr:NRAS* fish were *crestin:EGFP* positive (Supp. Fig. 5). We verified this using flow cytometry by analyzing *casper;crestin:EGFP;mcr:NRAS;mitf:mCherry* fish at 4 and 20 weeks. None of the nine 4 week old fish analyzed had *mitf:mCherry/crestin:EGFP* positive melanocytes, as compared to 100% of the nine 20 week old fish (Supp. Fig. 6). Furthermore, we verified neural crest progenitor gene expression using qRT-PCR. RNA was collected from *casper;mcr:NRAS* tumors at 4, 8, and 20 weeks of age and from *mitfa:BRAF^{V600E};p53$^{-/-}$;nacre;mcr:Empty* at 20 weeks of age (Supp. Fig. 7). RNA from normal skin of wildtype zebrafish was used as a control for normalization. *crestin* expression was significantly higher in the 8 and 20 week *mcr:NRAS* melanomas relative to the 4 week tumors (Fig. 5A). Interestingly, 2 of the 8 fish evaluated at 4 weeks had similar *crestin* expression levels as the 8 and 20 week melanomas (average of 2.4 dCt at 4 weeks and 2.9 dCt at 8 and 20 weeks). Additionally, neural crest genes *sox10* and *dlx2a* were also increased in the 8 and 20 week tumors (Fig. 5B and C). The neural crest progenitor signature found in the 8 and 20 week melanomas was similar to the *mitfa:BRAF^{V600E};p53$^{-/-}$;nacre;mcr:Empty* melanomas, with *crestin* being more highly expressed in the *BRAF*-mutant melanomas (Fig. 5A-C). Previous studies show that both low and high levels of *mitfa* have been observed in human and zebrafish melanomas (Flaherty et al., 2012; Lister et al., 2013). We found that both *NRAS*- and *BRAF*-mutant melanomas highly express *mitfa* in our zebrafish model system (Fig. 5D). Together these data indicate that zebrafish *NRAS*-driven melanomas have reactivated the neural crest progenitor state.

3. Discussion

Here we describe a zebrafish system that models *NRAS*-driven melanoma. Expression of NRAS^{Q61R} in melanocytes induces the formation of large hyperpigmented tumors in developing zebrafish beginning at 4 weeks of age. At around 9–12 weeks of age, the tumors appear to undergo oncogenic transformation and give rise to malignant melanoma. These results demonstrate that NRAS has a biphasic role in melanocyte proliferation and tumor formation. In humans, *NRAS*-mutant melanomas have been shown to present with thicker tumors, higher rates of proliferation rates, and worse overall survival after the diagnosis of stage IV disease compared to *BRAF*-mutant melanoma (Devitt et al., 2011; Heppt et al., 2017; Jakob et al., 2012). Due to the rapid tumor development and similarities to human melanoma, the *mcr:NRAS* model described here can be used to investigate novel diagnostic and therapeutic targets for *NRAS*-driven melanoma.

Although the recent development of immunomodulatory therapies have shown promise in *NRAS*-mutant melanomas (Johnson et al., 2015), very few therapies have been developed that specifically target these patients. A recent phase 3 clinical trial for patients with *NRAS*-mutant melanoma showed that, although treatment with a MEK inhibitor significantly improved progression-free survival compared to chemotherapy, the overall survival remained unchanged (Dummer et al., 2017). Therefore, there is still a great need to develop novel therapies for *NRAS*-driven melanoma. The anti-arthritis drug Leflunomide was shown to inhibit neural crest development and, in combination with a BRAF^{V600E} inhibitor, suppressed melanoma growth both in vitro and in mouse xenograft models (White et al., 2011). Given our finding that neural crest progenitor state reactivation occurs in *NRAS*-driven melanoma, combinatorial inhibition of MEK and the neural crest progenitor state may help improve patient survival.

Previous studies have demonstrated that both human and *mitfa:BRAF^{V600E};p53$^{-/-}$* zebrafish melanoma express a neural crest gene signature (Kaufman et al., 2016; Rambow et al., 2015; White et al., 2011). Here we show that the neural crest genes *crestin*, *sox10*, *dlx2a*, and *mitfa* are also upregulated in a zebrafish model of *NRAS*-driven malignant melanoma. The reemergence of a neural crest progenitor state seems to occur in conjunction with malignant progression. We found that 4 week old *mcr:NRAS* fish had about 18% engraftment upon transplantation (2/11), histologically, about 19% of these fish had melanoma-like lesions (3/16), and 25% of these tumors had *crestin* expression detectible by qRT-PCR (2/8). These data suggest that *crestin* is active in the early stages of *NRAS*-mutated melanoma. Together, this provides further evidence that the neural crest progenitor state reemergence is a key event in melanoma formation.

The *mitfa:BRAF^{V600E};p53$^{-/-}$* and *mitfa:EGFP:NRAS^{Q61K};p53$^{-/-}$* zebrafish models were previously shown to generate tumors that

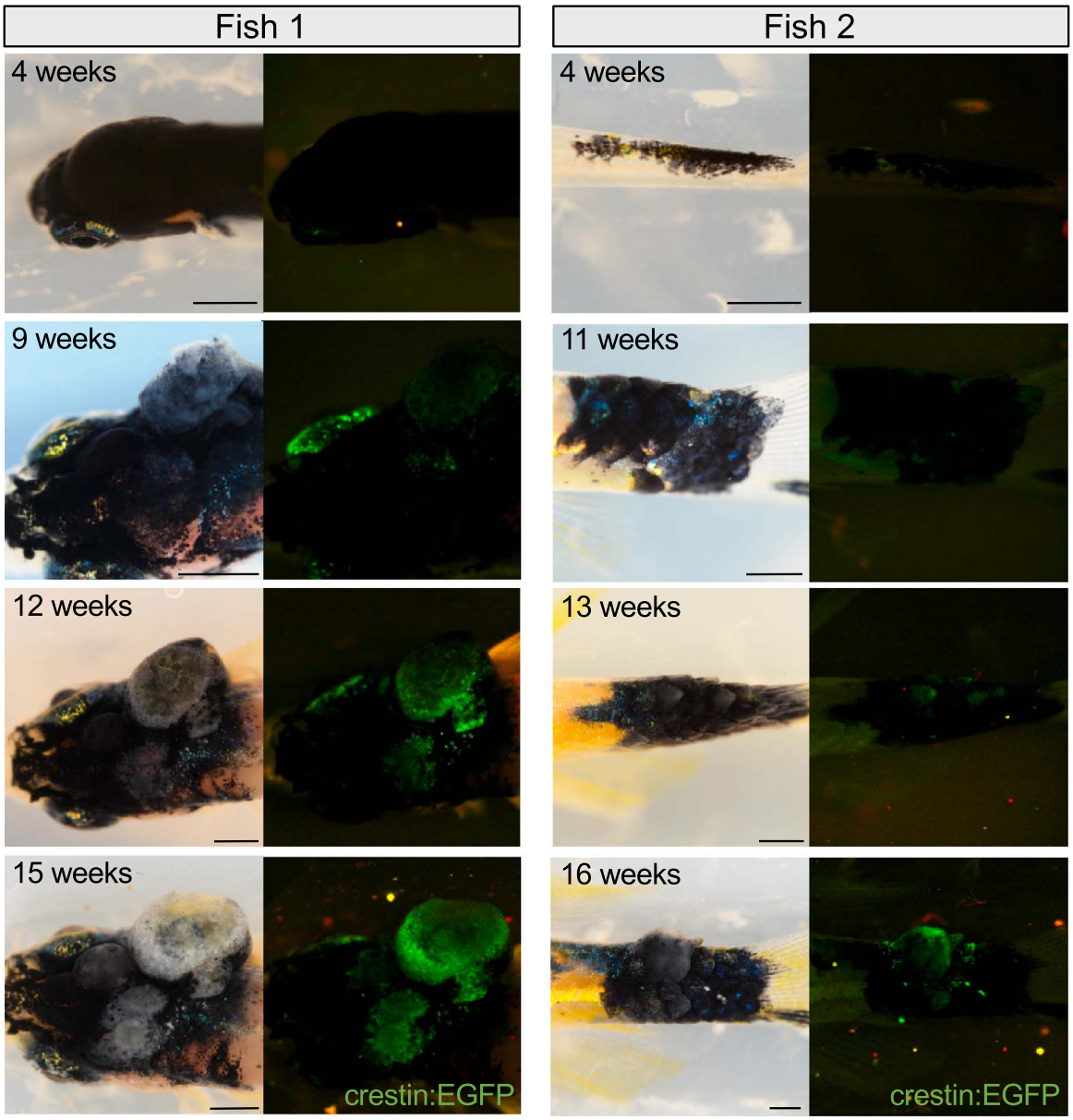

Fig. 4. *crestin:EGFP* turns on at 9–12 weeks of age. Two examples of *casper;mcr:NRAS;crestin:EGFP* zebrafish at 4–16 weeks post-fertilization. The *crestin:EGFP* transgene appears to be activated at between 9 and 12 weeks of age. Scale bars represent 1000 μm for all images.

pathologically resembled human melanoma (Dovey et al., 2009; Patton et al., 2005). In these stable lines, neither the *mitfa:BRAF*^{V600E} nor *mitfa:EGFP:NRAS*^{Q61K} alone were sufficient to generate melanomas. In our rapid transgenic model, we overexpress NRAS^{Q61R} in the rescued melanocytes of *casper* zebrafish. Despite wildtype levels of p53, malignant melanoma onset occurs at 9–12 weeks, which is substantially faster than the stable BRAF and NRAS p53-deficient lines (Dovey et al., 2009; Patton et al., 2005). The greatly accelerated tumor onset in the *mcr:NRAS* fish suggests that other aspects of the model, such as transient injection and melanocyte rescue, may account for this difference. Interestingly, the two previously generated *mitfa:EGFP:NRAS*^{Q61K} stable lines had widely varying copy numbers of the NRAS transgene, with one having significantly higher levels of the NRAS^{Q61K} transcript than the other (Dovey et al., 2009). Despite these differences, neither line developed tumors with wildtype levels of p53 and had similar rates of onset when p53 was lost, suggesting that the levels of NRAS might not play a major role in oncogenesis (Dovey et al., 2009). The formation of melanoma using only one oncogenic driver has been demonstrated previously in *kita*-GFP-HRAS zebrafish (Santoriello et al., 2010). The rapid onset time and high frequency of tumorigenesis suggests that NRAS is the sole driver of tumorigenesis in our model.

In our model system, the tumors that arise prior to malignant melanoma initiation do not express *crestin,* do not form tumors upon transplantation, and lack definitive cytomorphologic evidence of malignancy. These early tumors are reminiscent of giant Congenital Melanocytic Nevi (CMN), a benign melanocytic tumor that may cover a large area of the body. Although small and medium congenital nevi harbor both NRAS and BRAF mutations, 94.7% of giant CMNs contain a mutation in NRAS, with exome sequencing verifying that it is the sole recurrent somatic event driving CMN (Charbel et al., 2013). Patients with CMN have a significantly increased risk of developing melanoma proportional to the lesion size, reaching up to a 10% risk for lesions > 40 cm in diameter (Krengel et al., 2006). In our model, we see nearly 100% transformation of these lesions to melanomas. This suggests that the *mcr:NRAS* fish may represent a model to study the subset of

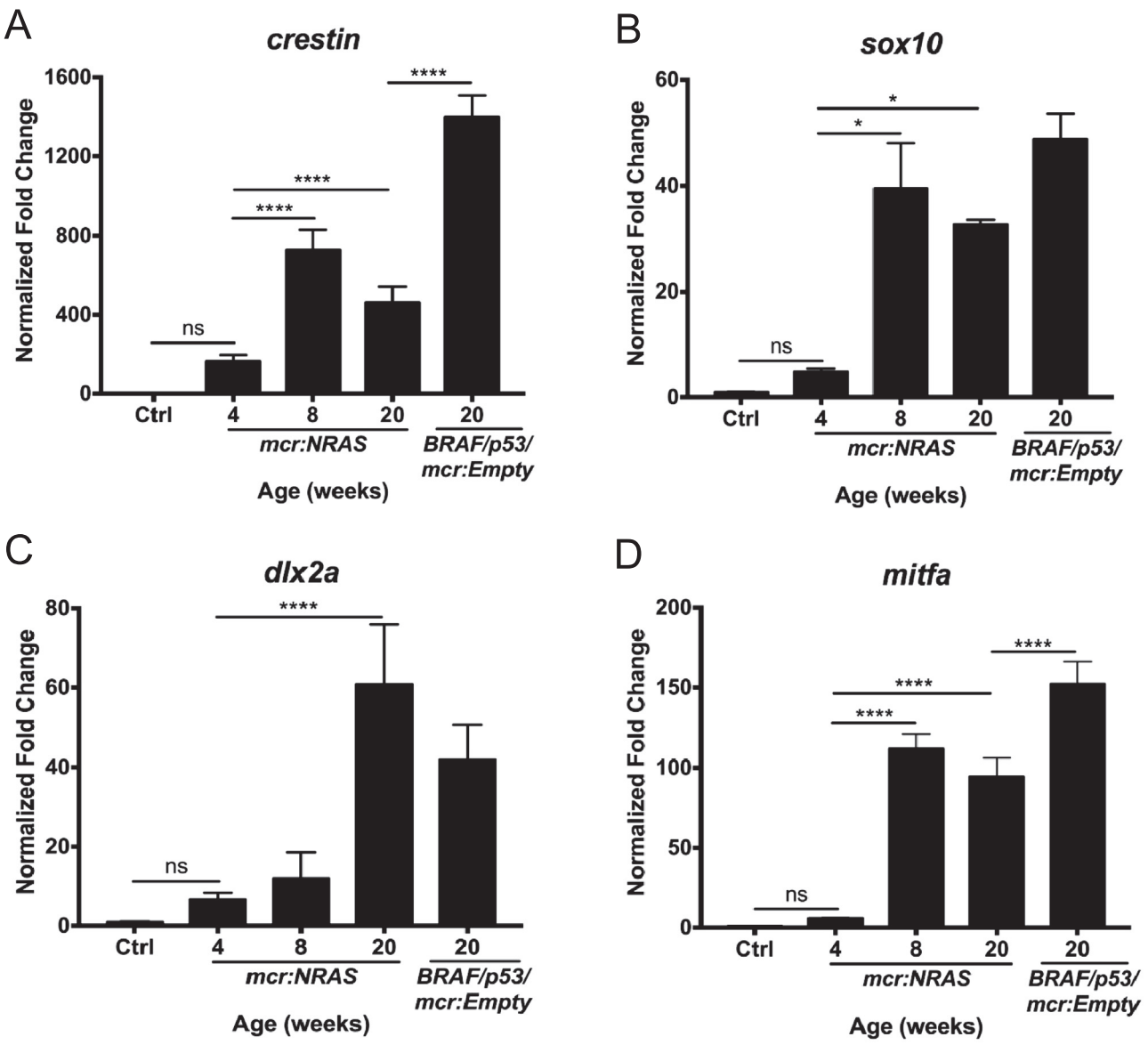

Fig. 5. *NRAS*-driven melanomas express a neural crest progenitor gene signature. (A-D) qRT-PCR results showing the neural crest genes *crestin, sox10, dlx2a,* and *mitfa*. ns=not significant; *p < 0.05; * ** *p < 0.0001 calculated using a two-way ANOVA with a Tukey's multiple comparisons test. n = 3–8 fish per condition.

patients with CMN that develop malignant melanomas from a pre-existing nevus.

These studies describe the evolution of *NRAS*-mutant melanoma in a novel zebrafish model system. Our data suggest that melanocytes in *mcr:NRAS* fish undergo a massive expansion beginning at around 2 weeks of age. This hyperproliferation results in the formation of a hyperpigmented benign nevus harboring the same mutation as the majority of CMN. We believe that some cells within the nevus then undergo oncogenic transformation, leading to the formation of malignant melanoma. The increase in neural crest progenitor genes coincides with transformation, indicating that reprogramming to a neural crest progenitor state plays a role in *NRAS*-driven melanoma initiation. Further studies are required to determine the precise molecular mechanisms driving this transformation event; however, we speculate that $NRAS^{Q61R}$ induces melanocytes to hyperproliferate and that neural crest progenitor reprogramming could enable them to overcome oncogenic senescence and undergo transformation. In conclusion, the *mcr:NRAS* model system reported here provides a rapid tool with which to study the role of neural crest reprogramming in melanoma initiation and identify novel therapies for *NRAS*-mutant malignant melanoma.

4. Materials and methods

4.1. Generation of mcr:NRAS zebrafish

The *NRAS* ORF was PCR-amplified from cDNA of SK-MEL-2 cells and topo-cloned into the pEntrD vector. A clone containing the Q61R mutation was identified by sequencing and used to generate the *mcr:NRAS* plasmid by Gateway reaction. *mcr:NRAS* was injected into either *casper*, *nacre*, or *casper;crestin:EGFP* zebrafish along with Tol2 mRNA at a concentration of 25 ng/μL. This study was performed in strict accordance with the recommendations in the Guide for the Care and Use of Laboratory Animals of the National Institutes of Health. The animal research protocol was approved by the Institutional Animal Care and Use Committee of Boston Children's Hospital. All zebrafish used in this study were maintained and euthanized under the guidelines of the Institutional Animal Care and Use Committee of Boston Children's Hospital.

4.2. Histology

Fish were euthanized and fixed in 4% paraformaldehyde overnight

at 4 °C. Paraffin embedding, sectioning, Hematoxylin and Eosin (H & E) staining were performed according to standard techniques by the Brigham & Women's Hospital Pathology Core. Histologic sections were reviewed by a pathologist (JKM) and classified as F-nevi when the tumors were composed of well differentiated pigmented melanocytes without overt cytologic atypia or evidence of local tissue invasion. Tumors were classified as MTIP lesions when they showed a pushing invasive front into underlying tissue with minimal cytologic atypia. In contrast, malignant melanomas were composed of well-to-poorly differentiated melanocytic tumors that showed variable amounts of pigmentation with an infiltrative/invasive growth pattern into adjacent tissues that often showed marked cytologic atypia characterized by cytomegaly, sometimes profound nuclear enlargement, and prominent nucleoli. Immunohistochemistry was performed with 5 µm thick formalin-fixed, paraffin-embedded tissue sections using the Leica Biosystems Bond III automated staining platform. Antibody Phospho ERK (p44/42 MAPK) from Cell Signaling Technologies, catalogue # 4370, clone D13.14.4E, was run at 1:500 dilution using the Leica Biosystems Refine Detection Kit with citrate antigen retrieval.

4.3. Imaging and quantitation

Zebrafish were anesthetized with 4% MS-222 (Western Chemical Incorporated) and imaged on a Nikon SMZ18 Stereomicroscope. Histological images were taken on an Olympus BX41 scope with an attached Olympus DP70 camera. Tumors categorized as MTIP or melanoma were measured for depth of invasion beneath the basement membrane underlying the mucosal surface of the fish in millimeters. Additionally, tumors were scored on an individual basis for predominant morphologic pattern (epithelioid, spindle cell, pleomorphic) and degree of cytologic atypia. In total, sixteen 4 week old fish, nine 8 week old fish, and twelve 20 week old fish were evaluated for histology.

4.4. Transplant

4.4.1. Preparation of mcr:NRAS donor material

The *mcr:NRAS* zebrafish were euthanized using ice, in accordance with the Boston Children's Hospital IACUC protocol. Early tumors (or pigmented lesions) were harvested from 4 week old *mcr:NRAS* using forceps and a scalpel under the Zeiss Discovery V8 Stereomicroscope. In parallel, established tumors were harvested from 20 week old *mcr:NRAS* zebrafish using forceps and a scalpel. We harvested tumors from three 20 week old donors and eleven 4 week old donors. The harvested tumor material was immediately placed in a 10 cm petri dish containing 2 mL of DMEM/F12 (Life Technologies), 10 × Penicillin Streptomycin (Life Technologies), 0.075 mg/mL of Liberase (Roche). The tumor material was incubated at room temperature for 30 min, and manually disaggregated with a clean razor every 10 min. Liberase was inactivated with the addition of 15 mL of buffer containing DMEM/F12 (Life Technologies), 10 × Penicillin Streptomycin (Life Technologies), and 15% heat-inactivated FBS (Life Technologies). A 40 µm filter (Becton Dickinson) was used to filter the resuspended tumor cells into a conical. Total cell numbers were calculated using a hemocytometer and the tumor cell suspension was centrifuged at 500 rcf for 5 min.

4.4.2. Transplantation of mcr:NRAS donor material into casper recipients

Adult casper fish were sub-lethally irradiated at 30 Gy split over 2 days and housed in isolation tanks. The recipients were anesthetized using 4% MS-222 (Western Chemical Incorporated) from a 4 g/L stock in a light-protected bottle. The anesthetized recipients were placed on a damp sponge and subcutaneously transplanted using a beveled 26 G Hamilton syringe (Hamilton) with 3 µL of 100k tumor cells in the dorsal cavity. Each donor tumor went into 3–5 recipients. The transplanted recipients were immediately placed in an isolated recovery tank and monitored daily with water changes. Tumor engraftment was assessed 14 days and 21 days post transplantation. Each data point on the graph in Fig. 3B and Supp. Fig. 4A represents the average tumor area for the 3–5 recipient fish for each donor.

4.5. FACS analysis

Single cell *casper;crestin:EGFP* embryos were injected with *mitf:mCherry* and *mcr:NRAS* along with Tol2 mRNA at a concentration of 25 ng/µL. Nine 4 week old and nine 20 week old *casper;crestin:EGFP;mitf:mCherry;mcr:NRAS* fish were sacrificed FACS analysis. A single gross tumor from each of the 20 week old fish and the whole body of 4 week old fish were individually chopped for 1–2 min. The finely chopped tissue was suspended in 3 mLs of TrypLE Express (ThermoFisher Scientific) and incubated at 37 °C shaking at 300 rpm for 30 min. Samples were filtered through a 40 µm filter and washed with 5 mL of FACS buffer, consisting of DPBS (Life Technologies), 10 × Penicillin Streptomycin (Life Technologies), and 2% heat-inactivated FBS (Life Technologies). Samples were centrifuged at 500 rcf for 5 min and resuspended in 150 µL FACS buffer. Samples were stained with SYTOX blue (ThermoFisher) immediately before sorting and analyzed for live (SYTOX blue negative), EGFP and/or mCherry positive cells on a FACSAria II (BD Biosciences).

4.6. qRT-PCR

Tumors were removed from 4, 8, and 20 week old *casper;mcr:NRAS* fish and 20 week *mitfa:BRAF^{V600E};p53$^{-/-}$;nacre;mcr:Empty* fish. Wild type zebrafish skin was used as a normalization control. Total RNA was isolated using the Qiagen RNeasy Mini Kit. First strand complementary DNA was synthesized from 500 ng of total RNA in a 20 µL reaction using SuperScript III Reverse Transcriptase (Invitrogen). Quantitative Real-time PCR was performed with C1000 thermocycler (Bio-Rad) using the SYBR GreenER qPCR SuperMix (Invitrogen). Primer sequences are presented in Supplementary Table 1. For each experimental sample, ΔCT was calculated by subtracting the CT value for b-actin from the CT value for the target gene. ΔΔCT was then calculated for every gene by dividing the ΔCT of the average wild type skin by the ΔCT of the sample.

4.7. Statistics

A log rank Mantel-Cox test was used to analyze statistical significance in tumor-free survival curves. For multi-group analysis, such as the depth of invasion at multiple weeks, a one-way ANOVA was used. A two-way ANOVA was used for grouped analysis of transplant engraftment area taken over two time points. For comparisons between transplant engraftment area, an unpaired *t*-test was used. A two-way ANOVA with Tukey's multiple comparisons test was used to compare between multiple time points and across multiple genes in the qRT-PCR analysis. The calculations were performed using GraphPad Prism 7 (GraphPad Software).

Acknowledgements

We would like to thank Charles Kaufman for providing the *crestin:EGFP* plasmid; Scott Granter for assistance in evaluating histology; Christian Lawrence, Kara Maloney, and Li-Kun Zhang for expert fish care; and Megan Insco, Haley Noonan, and Maurizio Fazio for helpful discussions regarding this manuscript. This research was supported by the Charles S Memorial Sloan Kettering Starr Foundation Cancer Consortium, R01CA103846-14, and T32HL007627.

Declarations of interest

None.

Appendix A. Supporting information

Supplementary data associated with this article can be found in the online version at doi:10.1016/j.ydbio.2018.05.026.

References

Akbani, R., Akdemir, K.C., Aksoy, B.A., Albert, M., Ally, A., Amin, S.B., Arachchi, H., Arora, A., Auman, J.T., Ayala, B., Baboud, J., Balasundaram, M., Balu, S., Barnabas, N., Bartlett, J., Bartlett, P., Bastian, B.C., Baylin, S.B., Behera, M., Belyaev, D., Benz, C., Bernard, B., Beroukhim, R., Bir, N., Black, A.D., Bodenheimer, T., Boice, L., Boland, G.M., Bono, R., Bootwalla, M.S., Bosenberg, M., Bowen, J., Bowlby, R., Bristow, C.A., Brockway-Lunardi, L., Brooks, S.B., Brzezinski, J., Bshara, W., Buda, E., Burns, W.R., Butterfield, Y.S.N., Button, M., Calderone, T., Cappellini, G.A., Carter, C., Carter, S.L., Cherney, L., Cherniack, A.D., Chevalier, A., Chin, L., Cho, J., Cho, R.J., Choi, Y., La, Chu, A., Chudamani, S., Cibulskis, K., Ciriello, G., Clarke, A., Coons, S., Cope, L., Crain, D., Curley, E., Danilova, L., D'Atri, S., Davidsen, T., Davies, M.A., Delman, K.A., Demchok, J.A., Deng, Q.A., Deribe, Y.L., Dhalla, N., Dhir, R., Dicara, D., Dinikin, M., Dubina, M., Ebrom, J.S., Egea, S., Eley, G., Engel, J., Eschbacher, J.M., Fedosenko, K.V., Felau, I., Fennell, T., Ferguson, M.L., Fisher, S., Flaherty, K.T., Frazer, S., Frick, J., Fulidou, V., Gabriel, S.B., Gao, J., Gardner, J., Garraway, L.A., Gastier-Foster, J.M., Gaudioso, C., Gehlenborg, N., Genovese, G., Gerken, M., Gershenwald, J.E., Getz, G., Gomez-Fernandez, C., Gribbin, T., Grimsby, J., Gross, B., Guin, R., Gutschner, T., Hadjipanayis, A., Halaban, R., Hanf, B., Haussler, D., Haydu, L.E., Hayes, D.N., Hayward, N.K., Heiman, D.I., Herbert, L., Herman, J.G., Crain, P., Hoadley, K.A., Hodis, E., Holt, R.A., Hoon, D.S., Hoppough, S., Hoyle, A.P., Huang, F.W., Huang, M., Huang, S., Hutter, C.M., Ibbs, M., Iype, L., Jacobsen, A., Jakrot, V., Janning, A., Jeck, W.R., Jefferys, S.R., Jensen, M.A., Jones, C.D., Jones, S.J.M., Ju, Z., Kakavand, H., Kang, H., Kefford, R.F., Khuri, F.R., Kim, J., Kirkwood, J.M., Klode, J., Korkut, A., Korski, K., Krauthammer, M., Kucherlapati, R., Kwong, L.N., Kycler, W., Ladanyi, M., Lai, M., Laird, P.W., Lander, E., Lawrence, M.S., Lazar, A.J., Aniak, R., Lee, D., Lee, J.E.J., Lee, J.E.J., Lee, K., Lee, S., Lee, W., Leporowska, E., Leraas, K.M., Li, H.I., Lichtenberg, T.M., Lichtenstein, L., Lin, P., Ling, S., Liu, J., Liu, O., Liu, W., Bodenheimer, G.V., Lu, Y., Ma, S., Ma, Y., Mackiewicz, A., Mahadeshwar, H.S., Malke, J., Mallery, D., Manikhas, G.M., Mann, G.J., Marra, R., Matejka, B., Mayo, M., Mehrabi, S., Meng, S., Meyerson, M., Mieczkowski, P.A., Miller, J.P., Miller, M.L., Mills, G.B., Moiseenko, F., Moore, R.A., Morris, S., Morrison, C., Morton, D., Moschos, S., Mose, L.E., Muller, F.L., Mungall, A.J., Albert, D., Murawa, P., Murray, B.A., Nezi, L., Ng, H., Nicholson, D., Noble, M.S., Osunkoya, A., Owonikoko, T.K., Ozenberger, B.A., Pagani, E., Paklina, O.V., Pantazi, A., Parfenov, M., Parfitt, J., Park, P.J., Park, W.Y., Parker, J.S., Passarelli, F., Penny, R., Perou, C.M., Pihl, T.D., Potapova, O., Prieto, V.G., Protopopov, A., Quinn, M.J., Radenbaugh, A., Rai, K., Ramalingam, S.S., Raman, A.T., Ramirez, N.C., Ramirez, R., Rao, U., Rathmell, W.K., Ren, X., Reynolds, S.M., Roach, J., Robertson, A.G., Ross, M.I., Roszik, J., Russo, G., Saksena, G., Saller, C., Samuels, Y., Sander, C.C., Sander, C.C., Sandusky, G., Santoso, N., Saul, M., Saw, R.P., Schadendorf, D., Schein, J.E., Schultz, N., Schumacher, S.E., Schwallier, C., Scolyer, J., Seidman, J., Sekhar, P.C., Sekhon, H.S., Senbabaoglu, Y., Seth, S., Shannon, K.F., Sharpe, S., Sharpless, N.E., Shaw, K.R.M., Shelton, C., Shelton, T., Shen, R., Sheth, M., Shi, Y., Shiau, C.J., Shmulevich, I., Sica, G.L., Simons, J.V., Sinha, R., Sipahimalani, P., Sofia, H.J., Soloway, M.G., Song, X., Sougnez, C., Korkut, A.J., Spycha??a, A., Stretch, J.R., Stuart, J., Suchorska, W.M., Sucker, A., Sumer, S.O., Sun, Y., Synott, M., Tabak, B., Tabler, T.R., Tam, A., Tan, D., Tang, J., Tarnuzzer, R., Tarvin, K., Tatka, H., Taylor, B.S., Teresiak, M., Thiessen, N., Thompson, J.F., Thorne, L., Thorsson, V., Trent, J.M., Triche, T.J., Tsai, K.Y., Tsou, P., Van Den Berg, D.J., Van Allen, E.M., Veluvolu, U., Verhaak, R.G., Voet, D., Voronina, O., Walter, D., Walton, J.S., Wan, Y., Wang, Y., Wang, Z., Waring, S., Watson, I.R., Weinhold, N., Weinstein, J.N., Weisenberger, D.J., White, P., Wilkerson, M.D., Wilmott, J.S., Wise, L., Wiznerowicz, M., Woodman, S.E., Wu, C.C.C.J., Wu, C.C.C.J., Wu, J., Wu, Y., Xi, R., Xu, A.W., Yang, D., Yang, L.L., Yang, L.L., Zack, T.I., Zenklusen, J.C., Zhang, H., Huang, J., Zhang, W., Zhao, X., Zhu, J., Zhu, K., Zimmer, L., Zmuda, E., Zou, L., Network, C.G.A., 2015. Genomic classification of cutaneous melanoma. Cell 161, 1681–1696. http://dx.doi.org/10.1016/j.cell.2015.05.044.

Ceol, C.J., Houvras, Y., Jane-Valbuena, J., Bilodeau, S., Orlando, D.A., Battisti, V., Fritsch, L., Lin, W.M., Hollmann, T.J., Ferré, F., Bourque, C., Burke, C.J., Turner, L., Uong, A., Johnson, L.A., Beroukhim, R., Mermel, C.H., Loda, M., Ait-Si-Ali, S., Garraway, L.A., Young, R.A., Zon, L.I., 2011. The histone methyltransferase SETDB1 is recurrently amplified in melanoma and accelerates its onset. Nature 471, 513–517. http://dx.doi.org/10.1038/nature09806.

Charbel, C., Fontaine, R.H., Malouf, G.G., Picard, A., Kadlub, N., El-Murr, N., How-Kit, A., Su, X., Coulomb-L & apos, Hermine, A., Tost, J., Mourah, S., Aractingi, S., Guegan, S., 2013. NRAS mutation is the sole recurrent somatic mutation in large congenital melanocytic nevi. J. Investig. Dermatol.. http://dx.doi.org/10.1038/jid.2013.429.

Devitt, B., Liu, W., Salemi, R., Wolfe, R., Kelly, J., Tzen, C.Y., Dobrovic, A., Mcarthur, G., 2011. Clinical outcome and pathological features associated with NRAS mutation in cutaneous melanoma. Pigment Cell Melanoma Res. 24, 666–672. http://dx.doi.org/10.1111/j.1755-148X.2011.00873.x.

Dovey, M., White, R.M., Zon, L.I., 2009. Oncogenic NRAS cooperates with p53 loss to generate melanoma in zebrafish. Zebrafish 6, 397–404. http://dx.doi.org/10.1089/zeb.2009.0606.

Dummer, R., Schadendorf, D., Ascierto, P.A., Arance, A., Dutriaux, C., Di Giacomo, A.M., Rutkowski, P., Del Vecchio, M., Gutzmer, R., Mandala, M., Thomas, L., Demidov, L., Garbe, C., Hogg, D., Liszkay, G., Queirolo, P., Wasserman, E., Ford, J., Weill, M., Sirulnik, L.A., Jehl, V., Bozón, V., Long, G.V., Flaherty, K., 2017. Binimetinib versus dacarbazine in patients with advanced NRAS-mutant melanoma (NEMO): a multicentre, open-label, randomised, phase 3 trial. Lancet Oncol. 18, 435–445. http://dx.doi.org/10.1016/S1470-2045(17)30180-8.

Flaherty, K.T., Hodi, F.S., Fisher, D.E., 2012. From genes to drugs: targeted strategies for melanoma. Nat. Rev. Cancer 12, 349–361. http://dx.doi.org/10.1038/nrc3218.

Heppt, M.V., Siepmann, T., Engel, J., Schubert-Fritschle, G., Eckel, R., Mirlach, L., Kirchner, T., Jung, A., Gesierich, A., Ruzicka, T., Flaig, M.J., Berking, C., 2017. Prognostic significance of BRAF and NRAS mutations in melanoma: a German study from routine care. BMC Cancer 17, 536. http://dx.doi.org/10.1186/s12885-017-3529-5.

Jakob, J.A., Bassett, R.L., Ng, C.S., Curry, J.L., Joseph, R.W., Alvarado, G.C., Rohlfs, M.L., Richard, J., Gershenwald, J.E., Kim, K.B., Lazar, A.J., Hwu, P., Davies, M.A., 2012. NRAS mutation status is an independent prognostic factor in metastatic melanoma. Cancer 118, 4014–4023. http://dx.doi.org/10.1002/cncr.26724.

Johnson, D.B., Lovly, C.M., Flavin, M., Panageas, K.S., Ayers, G.D., Zhao, Z., Iams, W.T., Colgan, M., DeNoble, S., Terry, C.R., Berry, E.G., Iafrate, A.J., Sullivan, R.J., Carvajal, R.D., Sosman, J.A., 2015. Impact of NRAS mutations for patients with advanced melanoma treated with immune therapies. Cancer Immunol. Res. 3, 288–295. http://dx.doi.org/10.1158/2326-6066.CIR-14-0207.

Johnson, D.B., Puzanov, I., 2015. Treatment of NRAS-mutant melanoma. Curr. Treat. Options Oncol., 16. http://dx.doi.org/10.1007/s11864-015-0330-z.

Kaufman, C.K., Mosimann, C., Fan, Z.P.Z.P., Yang, S., Thomas, A.J., Ablain, J., Tan, J.L., Fogley, R.D., van Rooijen, E., Hagedorn, E.J., Ciarlo, C., White, R.M., Matos, D.A., Puller, A.-C.A.-C., Santoriello, C., Liao, E.C., Young, R.A., Zon, L.I., 2016. A zebrafish melanoma model reveals emergence of neural crest identity during melanoma initiation. Science 351. http://dx.doi.org/10.1126/science.aad2197, (aad2197-aad2197).

Krengel, S., Hauschild, A., Schäfer, T., 2006. Melanoma risk in congenital melanocytic naevi: a systematic review. Br. J. Dermatol. 155, 1–8. http://dx.doi.org/10.1111/j.1365-2133.2006.07218.x.

Kwan, K.M., Fujimoto, E., Grabher, C., Mangum, B.D., Hardy, M.E., Campbell, D.S., Parant, J.M., Yost, H.J., Kanki, J.P., Chien, C.-B., 2007. The Tol2kit: a multisite gateway-based construction kit for Tol2 transposon transgenesis constructs. Dev. Dyn. 236, 3088–3099. http://dx.doi.org/10.1002/dvdy.21343.

Lister, J.A., Capper, A., Zeng, Z., Mathers, M.E., Richardson, J., Paranthaman, K., Jackson, I.J., Patton, E.E., 2013. A Conditional zebrafish MITF mutation reveals MITF levels are critical for melanoma promotion vs. regression in vivo. J. Investig. Dermatol. 134, 133–140. http://dx.doi.org/10.1038/jid.2013.293.

Patton, E.E., Widlund, H.R., Kutok, J.L., Kopani, K.R., Amatruda, J.F., Murphey, R.D., Berghmans, S., Mayhall, E.A., Traver, D., Fletcher, C.D.M.M., Aster, J.C., Granter, S.R., Look, A.T., Lee, C., Fisher, D.E., Zon, L.I., 2005. BRAF mutations are sufficient to promote nevi formation and cooperate with p53 in the genesis of melanoma. Curr. Biol. 15, 249–254. http://dx.doi.org/10.1016/j.cub.2005.01.031.

Rambow, F., Job, B., Petit, V., Gesbert, F., Delmas, V., Seberg, H., Meurice, G., Van Otterloo, E., Dessen, P., Robert, C., Gautheret, D., Cornell, R.A., Sarasin, A., Larue, L., 2015. New functional signatures for understanding melanoma biology from tumor cell lineage-specific analysis. Cell Rep., 1–15. http://dx.doi.org/10.1016/j.celrep.2015.09.037.

Santoriello, C., Gennaro, E., Anelli, V., Distel, M., Kelly, A., Köster, R.W., Hurlstone, A., Mione, M., 2010. Kita driven expression of oncogenic HRAS leads to early onset and highly penetrant melanoma in zebrafish. PLoS One 5, e15170. http://dx.doi.org/10.1371/journal.pone.0015170.

Siegel, R.L., Miller, K.D., Jemal, A., 2016. Cancer statistics. CA Cancer J. Clin. 66, 7–30. http://dx.doi.org/10.3322/caac.21332.

Uribe, P., Andrade, L., Gonzalez, S., 2006. Lack of association between BRAF mutation and MAPK ERK activation in melanocytic nevi. J. Investig. Dermatol. 126, 161–166. http://dx.doi.org/10.1038/sj.jid.5700011.

White, R.M., Cech, J., Ratanasirintrawoot, S., Lin, C.Y., Rahl, P.B., Burke, C.J., Langdon, E., Tomlinson, M.L., Mosher, J., Kaufman, C., Chen, F., Long, H.K., Kramer, M., Datta, S., Neuberg, D., Granter, S., Young, R.A., Morrison, S., Wheeler, G.N., Zon, L.I., 2011. DHODH modulates transcriptional elongation in the neural crest and melanoma. Nature 471, 518–522. http://dx.doi.org/10.1038/nature09882.

White, R.M., Sessa, A., Burke, C., Bowman, T., LeBlanc, J., Ceol, C., Bourque, C., Dovey, M., Goessling, W., Burns, C.E., Zon, L.I., 2008. Transparent adult zebrafish as a tool for in vivo transplantation analysis. Cell Stem Cell 2, 183–189, (https://doi.org/S1934-5909)(07)(00275-5)(pii)(10.1016/j.stem.2007.11.002).